TU Delft

Delft University of Technology

Acoustic Noise Analysis of Interior Permanent Magnet Synchronous Machine for Electric Vehicle Application

Son, Changbum; Dong, Jianning; Bauer, Pavol

DOI
10.1109/ITEC48692.2020.9161383

Publication date
2020

Document Version
Final published version

Published in
2020 IEEE Transportation Electrification Conference & Expo (ITEC)

Citation (APA)
Son, C., Dong, J., & Bauer, P. (2020). Acoustic Noise Analysis of Interior Permanent Magnet Synchronous Machine for Electric Vehicle Application. In *2020 IEEE Transportation Electrification Conference & Expo (ITEC)* (pp. 450-455). IEEE. https://doi.org/10.1109/ITEC48692.2020.9161383

Important note
To cite this publication, please use the final published version (if applicable).
Please check the document version above.

Copyright
Other than for strictly personal use, it is not permitted to download, forward or distribute the text or part of it, without the consent of the author(s) and/or copyright holder(s), unless the work is under an open content license such as Creative Commons.

Takedown policy
Please contact us and provide details if you believe this document breaches copyrights.
We will remove access to the work immediately and investigate your claim.

This work is downloaded from Delft University of Technology.
For technical reasons the number of authors shown on this cover page is limited to a maximum of 10.

Green Open Access added to TU Delft Institutional Repository

'You share, we take care!' - Taverne project

https://www.openaccess.nl/en/you-share-we-take-care

Otherwise as indicated in the copyright section: the publisher is the copyright holder of this work and the author uses the Dutch legislation to make this work public.

Acoustic Noise Analysis of Interior Permanent Magnet Synchronous Machine for Electric Vehicle Application

Changbum Son, Jianning Dong* and Pavol Bauer
Department of Electrical Sustainable Energy, Delft University of Technology
Delft, The Netherlands
*Email: J.Dong-4@tudelft.nl

***Abstract*—This paper analyses the electromagnetic resulted acoustic noise of an interior permanent magnet synchronous machine (IPMSM). The influences of electromagnetic nonlinearity, pulse-width-modulation (PWM) and motor frame on the acoustic noise are considered. A finite element model is used to extract the look up tables (LUTs) of flux linkage and air gap electromagnetic force distributions as functions of rotor positions and excitation currents. Based on the generated LUTs, an electrical dynamic model is used to simulate stator current and air gap electromagnetic force waveforms considering PWM. Simulated forces are fed to a lumped parameter mechanical model to predict the acoustic noise of the IPMSM in a wide operation range. In the end, a structural method and a PWM based method are proposed to reduce the noise level of the IPMSM. Simulation results show changing the frame thickness and adopting a different PWM method can effectively mitigate the noisy operating points.**

***Index Terms*—acoustic noise, interior permanent magnet machine, vibration, pulse width modulation**

I. Introduction

Electrical vehicles (EV) are inevitably taking over traditional internal combustion engine (ICE) powered vehicles. As a consequence, the source of noise is also changing from ICE to electric motors. Although the EV motors are "quieter" than ICE as people may think, the noises and vibrations brought by the rapidly changing electromagnetic force and the fast switching motor drives may affect the driving experience, human health and the lifetime of the power train, especially when motors with high power density are used [1], [2].

Interior permanent magnet synchronous machines (IPMSMs) are extensively used in electric vehicles (EVs) because its high power density, high efficiency and its capability to operate in wide speed range. In the meanwhile, the high power density and complex magnetic circuits of IPMSMs bring potential acoustic noise problems, which is of particular interest in the EV industry [3], [4]. In order to predict the acoustic behaviour of the IPMSM accurately, different aspects affecting the dynamic performances have to be considered: the nonlinearity of the magnetic circuit, the mechanical dynamics of the stator and motor frame, and the pulse-width-modulation (PWM) of the voltage source inverter [1], [3]–[5].

Both analytical analysis and multi-physical numerical simulation can be used to address the above aspects for IPMSM acoustic noise prediction. The analytical methods are able to predict the air-gap flux density and hence the air-gap force, and the natural frequency of simple frames by making certain assumptions [6]–[8]. However, analytical models are difficult to obtain accurate results when electromagnetic nonlinearity and structural complexity are not negligible, which is the case for IPMSM. Numerical simulations are able to deliver accurate results considering real geometries and nonlinearity, but its computation time increases exponentially when the PWM switching is modelled [4], [5], [9], [10].

This paper uses a simplified hybrid methodology to predict the acoustic noise of IPMSMs. First a 2D static finite element model is used to generate the flux linkage look up tables (LUTs) and air gap force LUTs of the IPMSM in the dq reference frame. Then the LUTs are used to construct an electrical dynamic model to obtain current waveforms and air gap radial force waveforms in a wide operation range. Then the simulated results are fed to an analytical mechanical dynamic model to predict the acoustic noise behaviour. The methodology is applied to an IPMSM designed for a battery EV. Based on the obtained results, a structural method and a PWM method are proposed respectively to reduce the overall noise level of the IPMSM. Main parameters and the finite element analysis (FEA) model of the investigated IPMSM [11] are shown in Table I and Figure 1 respectively.

TABLE I
Main Parameters of Investigated IPMSM

Parameters	Values
Rated power	80 kW
Top speed	10 krpm
Number of poles	8
Stator outer diameter	200 mm
Frame thickness	30 mm
Air-gap length	0.5 mm
Stator stack length	151 mm
Drive method	PWM controlled VSI
Switching frequency	5 kHz

II. Analysis Methodology

A. Hybrid Noise Calculation

The IPMSM used in EV applications is often fed by the voltage source inverter (VSI), which will introduce current

Authorized licensed use limited to: TU Delft Library. Downloaded on September 06,2021 at 12:49:41 UTC from IEEE Xplore. Restrictions apply.

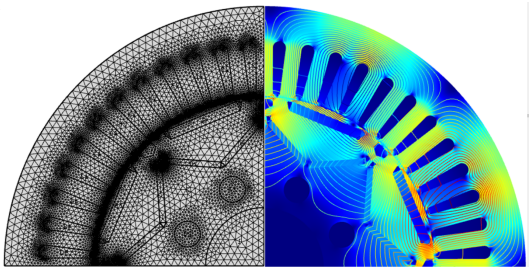

Fig. 1. FEA model of investigated IPMSM.

ripples and additional noise excitations. A hybrid method is used in this paper to analyse the noise performance of the IPMSM considering the influence of the VSI. Figure 2 compares the hybrid method used in this paper with the numerical method, where $p_{r,v_s}(i_{dq},\theta_r)$ is the LUT of the air gap radial force harmonics, $i_{dq,v_r}(\Psi_{dq})$ is the LUT of the current spatial harmonics in the dq reference frame, v_r and v_s are rotor and stator spatial harmonic orders, respectively. t is time and θ_r is the rotor electrical position.

In both methods, an electrical dynamic model including the PWM modulator, the VSI and the non-linear IPMSM model are needed to simulate the electrical dynamic performances at given speed and torque references. It utilizes spatial harmonics based flux linkage and air gap radial force LUTs to consider the nonlinearity and slotting effect [5], [7], as shown in Figure 3. It can also be replaced with two way coupled simulation in the numerical method, which makes it even more computation resources demanding and time consuming.

In the numerical method, the simulated current waveforms including the switching ripples are fed back to the transient electromagnetic FEA model to obtain the electromagnetic force on each node of the IPMSM FEA stator model in the time domain. The nodal force is then decomposed into the frequency components by applying the fast Fourier transformation (FFT), and mapped to a solid mechanical dynamic FEA model. The stator frame surface displacement computed from the solid mechanical model is coupled to an acoustic FEA model to simulate the acoustics noise behaviours.

The hybrid method replaces the most time consuming parts (transient electromagnetics FEA, mechanical dynamics FEA and acoustics FEA) with analytical models. The air-gap radial force wave is directly obtained from the LUTs in the electrical dynamic model, as shown in Figure 3, where $p_r(i_{dq},\theta_r)$ is the radial force LUT, R_s is the stator phase resistance, $\Psi_{\alpha\beta}$ and Ψ_{dq} are the flux linkage in respective reference frames, $i_{dq}(\Psi_{dq})$ is the current LUT, and p is the number of pole pairs.

B. Electromagnetic Dynamics Analysis

The electromagnetic model is implemented in COMSOL Multiphysics, as shown in Figure 1. Nonlinearity of the magnetic material is modelled in the model. A series of static FEA is carried out to obtain the dq flux linkage $\Psi_{dq}(i_{dq},\theta_r)$ LUT as functions of rotor position θ_r and the current vector i_{dq} in the dq reference frame. A mesh grid of 5×5 dq current pairs are used in the interested operation quarter for the static FEA, which is proved to be accurate enough.

In order to make the LUTs suitable for integral in the electrical dynamics simulation incorporating the PWM VSI, the $\Psi_{dq}(i_{dq},\theta_r)$ LUT is then inverted to a current vector LUTs $i_{dq}(\Psi_{dq},\theta_r)$ at each simulated rotor position θ_r. In order to reduce the size of the LUTs, computational resources for the interpolation and improve the accuracy, the $i_{dq}(\Psi_{dq},\theta_r)$ LUT is then decomposed into spatial harmonics $i_{dq,v_r}(\Psi_{dq})$. In this paper, rotor spatial harmonics up to ±12 are considered, as shown in Figure 3. To reduce the number of computations, the symmetry of the magnetic field is considered. Detailed method for the LUT construction and inversion can be found in [7].

A unique feature of the IPMSM is its reluctance torque. To use the reluctance torque sufficiently, maximum torque per ampere (MTPA) control is often used. After the $i_{dq,v_r}(\Psi_{dq})$ LUT is generated, an optimisation algorithm is used to search for optimal current pairs for certain torque references and speeds, considering the current and voltage constraints of the VSI. The generated LUTs can be used together with steady state machine equations to calculate the electromagnetic torque and phase voltage. The optimisation problem is described as follows: for a given T_e set point,

$$\begin{aligned} \underset{|i_{dq}|}{\text{minimize}} \quad & T_e = \frac{3}{2}\Psi_{dq,1}(i_{dq}) \times i_{dq} \\ \text{subject to} \quad & U_{ph} = \sqrt{(p\omega_m|\Psi_{dq,1}(i_{dq})|)^2 + R_s^2|i_{dq}|^2)} \le U_{max} \end{aligned} \tag{1}$$

where only the fundamental component of the flux linkage $\Psi_{dq,1}(i_{dq})$ is considered, T_e is the electromagnetic torque, ω_m is the mechanical speed of the IPMSM, U_{ph} and U_{max} are the phase peak voltage and the maximum phase peak voltage the inverter can supply. The search results are saved as a current reference table, which is used to feed the electrical dynamics model shown in Figure 3.

The test data of the investigated IPMSM summarized in [11] is used to validate the electromagnetic analysis. As shown in Figure 4, the simulated torque at various operating points is close to the test results, which validates the accuracy of the electromagnetic model.

The radial force waveform in the air gap is also obtained at the same time from the static FEA models at a series of i_{dq} excitations and rotor positions. Thus the $p_r(i_{dq},\theta_s,\theta_r)$ LUT is obtained. To improve the interpolation accuracy and reduce the LUT size, $p_r(i_{dq},\theta_s,\theta_r)$ is also decomposed into the stator spatial harmonic series $p_{r,v_s}(i_{dq},\theta_r)$. The spatial harmonic order v_s should be multiples of the greatest common divider (GCD) of number of stator slots and number of magnet poles. For the investigated IPMSM, v_s is 0, 8, 16, ...

The electrical dynamics model as shown in Figure 3 is implemented in MATLAB/Simulink to simulate the electromagnetic dynamics of the IPMSM. The $i_{dq,v}(\Psi_{dq})$ LUT is used to consider the electromagnetic nonlinearity and the spatial harmonics. The simulated output current and the rotor position are used to directly obtain the air gap radial force

Authorized licensed use limited to: TU Delft Library. Downloaded on September 06,2021 at 12:49:41 UTC from IEEE Xplore. Restrictions apply.

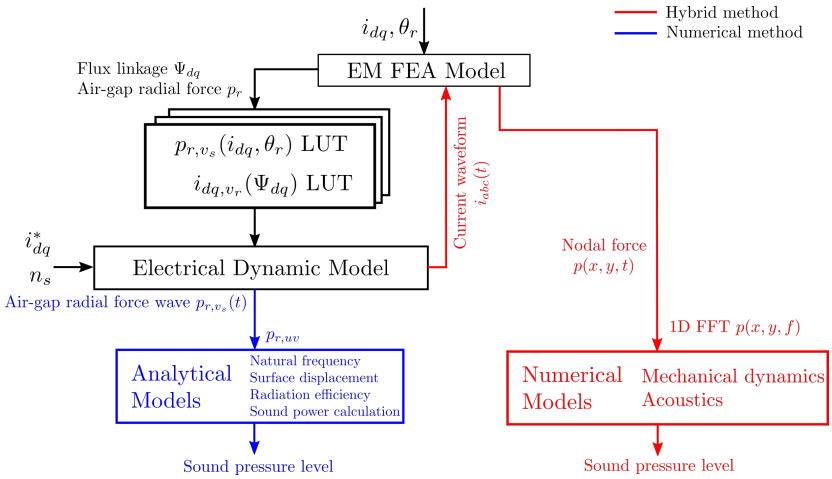

Fig. 2. Flow charts of the hybrid method and the numerical method.

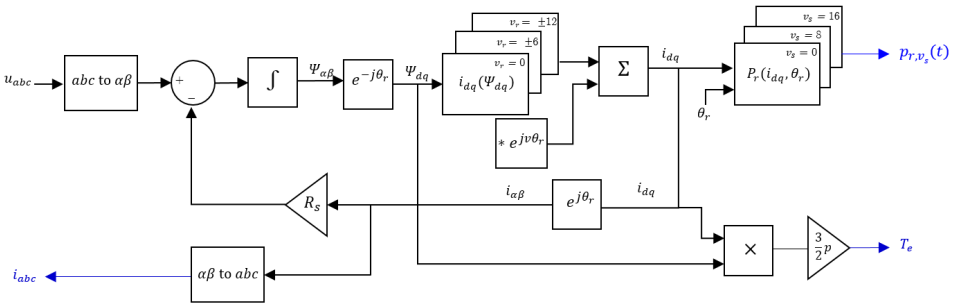

Fig. 3. Flow charts of the hybrid method and the numerical method.

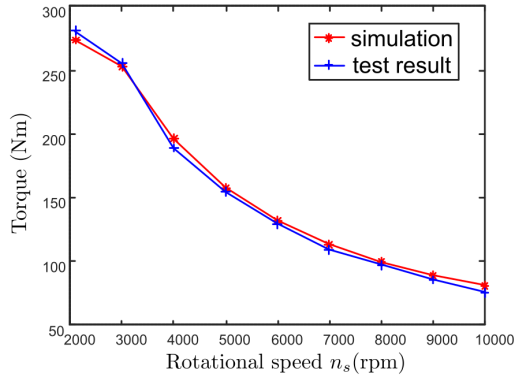

Fig. 4. Torque-speed curve comparison between the test results and the simulated results.

harmonics from the $p_{r,v_s}(i_{dq}, \theta_r)$ LUT via interpolation.

C. Mechanical Vibrations and Noise Radiation

In the mechanical vibration and noise radiation analysis, it is assumed that only radial force is contributing to vibrations and audible noises, which will neglect certain noises but is able to consider the main contributors [12]–[14].

The simulated radial force harmonics is changing with respect to the rotor position as the motor rotates. The obtained time changing radial force spatial harmonics are then further decomposed into spatial and time harmonics $p_{r,uv}$, where the subscript u and v denote for time harmonic order and spatial harmonic order respectively.

The mechanical vibrations and noises are calculated based on lumped parameter analytical models. Methods and models in [13] are used to calculate the natural frequency of different vibrations modes and surface displacements caused by different time/spatial harmonic pairs $p_{r,uv}$. In the lumped parameter mechanical models, the stator is modelled as a cylinder, while the stator teeth and windings considered as lumped mass which does not contribute to the stiffness of the stator. Detailed structure and fixature of the stator frame are not precisely modelled.

Only the circumferential modes are considered for the investigated IPMSM, interested vibrations modes of which are $m = 0$, $m = 8$, $m = 16$, $m = 24 \ldots$ etc. considering the force and structural symmetry. Table II shows the calculated natural frequencies of the stator. It can be seen that the natural frequency of mode $m = 0$ is close to the switching frequency region, and will contribute to significant noises. As the mode order getting higher, the natural frequency is higher, which results in a lower surface displacement and radiation efficiency [7], [15], and thus contribute less to noises.

After the natural frequencies and the surface displacement

Authorized licensed use limited to: TU Delft Library. Downloaded on September 06,2021 at 12:49:41 UTC from IEEE Xplore. Restrictions apply.

TABLE II
CALCULATED NATURAL FREQUENCIES OF DIFFERENT STATOR VIBRATION MODES

Vibration modes (m)	0	1	4	8
Natural Frequency (Hz)	7620	6410	8370	12040

are calculated, resulted noises caused by different harmonics can be quantified as sound power in the frequency domain by superimposing the contribution from each vibration mode m. Analytical modal sound radiation efficiency is used to calculate the modal sound power from the modal surface displacement [7], [13], [15].

III. RESULTS AND NOISE REDUCTION

A. Validation of Models

Numerical 2D electromagnetic model, 3D mechanical dynamics model and sound radiation model of the IPMSM are developed in COMSOL Multiphysics to validate the hybrid model used in the paper. Because of the limited computation resources, one way coupling is used between the models, and only sinusoidal excitation without PWM current ripples is modelled.

The torque-speed curve in Figure 4 is used to simulate an acceleration test. Figure 5 compares the waterfall plot of the average sound pressure level (SPL) at 1 m distance away from the IPMSM obtained from the hybrid method and the numerical method. It can be seen that the noisy regions predicted by both methods match up to each other. The most noisy lines, curve A in Figure 5(a) is slightly higher than that in Figure 5(b), which is because the analytically calculated $m = 0$ natural frequency is lower than that predicted from the numerical method. Compared to the analytical method, higher noise can be observed in the high speed, high frequency region C in Figure 5(b), which is because as frequency increases, wavelength of the sound is more comparable to the geometry of the machine, which decreases the accuracy of the lumped parameter method. However, the time spent on model preparation and computation is remarkably reduced.

It can be concluded that, although the hybrid method is not as accurate as the numerical method, it provides a fast approach to EV motor noise calculation with reasonable accuracy, especially when simulations on the influence of PWM and a wide range of operating points are needed. In practice, the accuracy of the hybrid method can be further improved by replacing the lumped parameter mechanical/sound models with numerically calculated or measured modal frequency response.

B. Results of the Original Design

Carrier based symmetrical PWM with zero sequence signal injection is modelled in the analysis [16]. The switching frequency is set at 5 kHz. A profile of the IPMSM accelerating from low speed using the maximum torque per ampere (MTPA) control to the field weakening region till the top speed using the torque reference shown in Figure 4 is simulated.

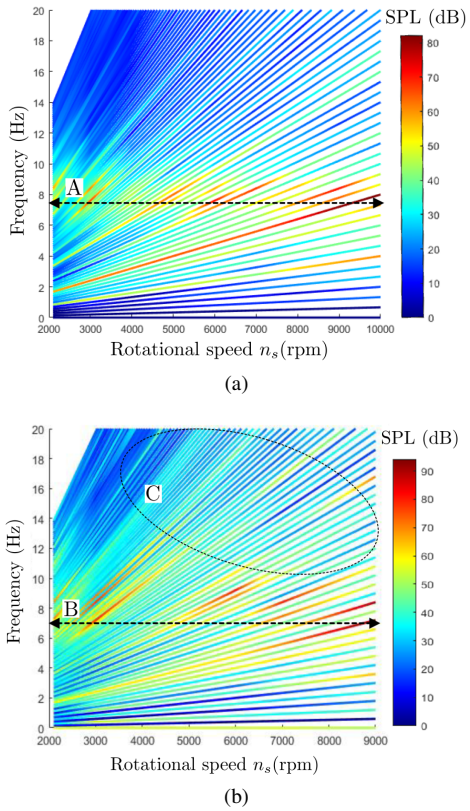

Fig. 5. Comparison between the results obtained from (a) the hybrid method and (b) the numerical method.

Figure 6 compares the SPL waterfall plots of the IPMSM with sinusoidal excitations with that of PWM excitations. From Figure 6(a) and (b), it can be seen that in both cases, the most noisy region is around 7620 Hz, which is corresponding to the $m = 0$ vibration mode of the stator. The maximum SPL is increased by almost 10 dB as a result of the PWM excitation. The highest SPL occurs at the high speed region in the sinusoidal case, which is of the same magnitude with corresponding region of the PWM case. In the PWM case, the SPL at low speed around 3000 rpm is the highest. High noise also exists at high frequencies compared with the sinusoidal case. For simplicity, Figure 6(c) presents the most dominant SPL components with PWM excitation. It can be seen that the switching related harmonics (red labels) resonant with mode $m = 0$ at low speed, while slotting harmonics (blue labels) resonant with mode $m = 0$ at high speed. Another interesting point in Figure 6(c) worth noting is that when speed is above 7000 rpm, the switching contribution tends to reduce, which is because of the over modulation.

Apparently, most of the noise comes from the resonance between the $m = 0$ vibration mode and the harmonics brought by either switching and slotting. Among them, the resonance at 3000 rpm is the most significant, which is close to the operation point of the EV in urban environment. In order to improve the acoustic noise performance of the IPMSM, two methods are proposed to suppress the noise.

Authorized licensed use limited to: TU Delft Library. Downloaded on September 06,2021 at 12:49:41 UTC from IEEE Xplore. Restrictions apply.

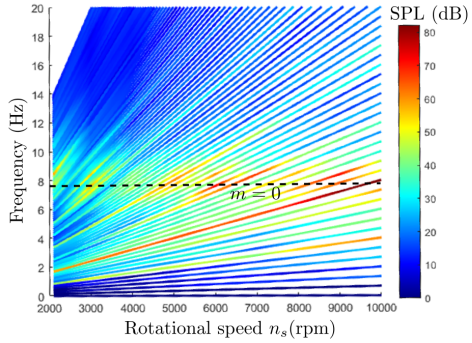

(a)

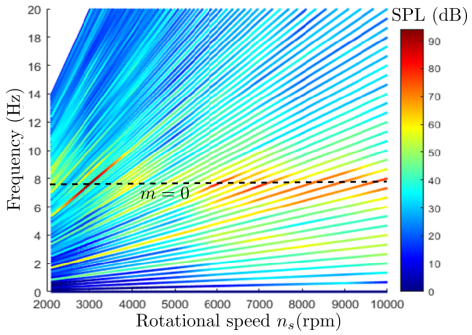

(b)

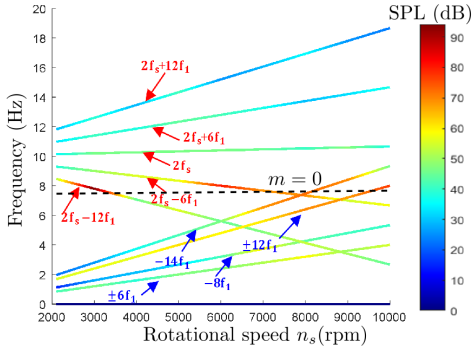

(c)

Fig. 6. Waterfall plot of calculated SPL: (a) sinusoidal excitation (b) PWM excitation (c) dominant SPL components under PWM excitation.

C. Noise Reduction

The first method (structure modification) is to increase the frame thickness from 30 mm to 52 mm, so that the natural frequency of mode $m = 0$ is increased from 7620 Hz to 8640 Hz. Figure 7 shows the SPL waterfall plot after the modification. Compared with Figure 6(b), it can bee seen that as the mode $m = 0$ natural frequency increases, the resonance occurs around 3000 rpm is suppressed. However, higher noise is introduced in the high frequency region at both low speed and high speed. Moreover, increasing thickness brings additional weight to the IPMSM.

The second method (PWM modification) is to use variable switching frequency. Instead of using a fixed switching frequency at 5 kHz, the frequency modulation ratio is kept at $m_f = 27$, so that the switching frequency is increasing from

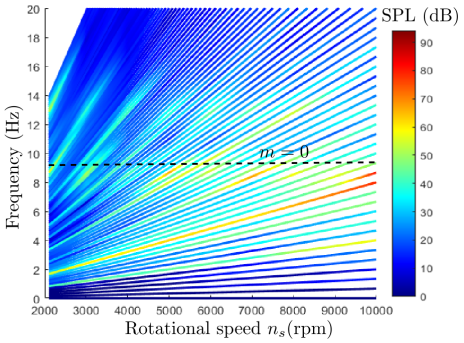

Fig. 7. Waterfall plot of calculated SPL after geometry modification.

low speed to high speed. Figure 8(a) compares the SPL spectra at 3000 rpm with that from the fixed switching frequency, clearly that switching harmonics still contribute the most to the noise. However, by shifting the switching frequency from 5 kHz to 5.4 kHz, the peak noise around the mode 0 natural frequency is reduced by around 20 dB. Compared the waterfall plot in Figure 8(b) with that in Figure 6(b), the SPL is reduced at both low speed region and high speed region, and the number of noisy regions are also reduced.

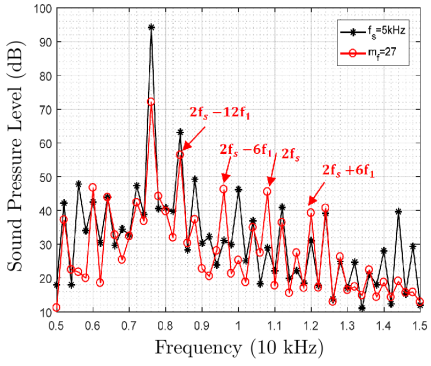

(a)

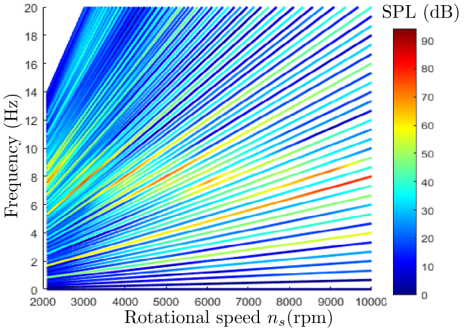

(b)

Fig. 8. SPL results with variable switching frequency: (a) spectra at 3000 rpm (b) waterfall plot.

IV. Conclusions

A simple hybrid method to predict electromagnetic resulted acoustic noise behaviours of the IPMSM has been presented

Authorized licensed use limited to: TU Delft Library. Downloaded on September 06,2021 at 12:49:41 UTC from IEEE Xplore. Restrictions apply.

in the paper by incorporating numerical models and analytical models. The method is applied to an IPMSM designed for battery EV. The calculated results are benchmarked by numerical simulations, showing reasonable accuracy. The method can be used for fast comparisons of noise performances of different design candidates and different control or PWM strategies. It is shown that among all the contribution factors, resonance between mode $m = 0$ and the PWM switching spectra contribute the most to the noise.

Both structure modification and PWM strategy modification are used to suppress the noise of the investigated IPMSM. Results show that modifying the PWM strategy can help mitigate the resonance and is more effective compared to structure modification and does not introduce additional weight.

REFERENCES

[1] A. Andersson, "Electric Machine Control for Energy Efficient Electric Drive Systems," PhD Thesis, Chalmers University of Technology, Gothenburg, Sweden, 2018.

[2] C. Ma, Q. Li, L. Deng, C. Chen, Q. Liu, and H. Gao, "A Novel Sound Quality Evaluation Method of the Diagnosis of Abnormal Noise in Interior Permanent-Magnet Synchronous Motors for Electric Vehicles," *IEEE Trans. Ind. Electron.*, vol. 64, no. 5, pp. 3883–3891, May 2017.

[3] J. Liang, Y. Li, C. Mak, B. Bilgin, D. Al-Ani, and A. Emadi, "A Comprehensive Analysis of the Acoustic Noise in an Interior Permanent Magnet Traction Motor," in *2019 IEEE Energy Conversion Congress and Exposition (ECCE)*, Sep. 2019, pp. 3845–3851, iSSN: 2329-3721.

[4] W. Deng and S. Zuo, "Electromagnetic Vibration and Noise of the Permanent-Magnet Synchronous Motors for Electric Vehicles: An Overview," *IEEE Trans. Transport. Electrific.*, vol. 5, no. 1, pp. 59–70, Mar. 2019.

[15] M. Boesing, M. Niessen, T. Lange, and R. De Doncker, "Modeling spatial harmonics and switching frequencies in PM synchronous machines and their electromagnetic forces," in *2012 XXth International Conference on Electrical Machines (ICEM)*, Sep. 2012, pp. 3001–3007.

[5] B. Bilgin, J. Liang, M. V. Terzic, J. Dong, R. Rodriguez, E. Trickett, and A. Emadi, "Modeling and Analysis of Electric Motors: State-of-the-Art Review," *IEEE Trans. Transport. Electrific.*, vol. 5, no. 3, pp. 602–617, Sep. 2019.

[6] B. Guo, Y. Huang, F. Peng, and J. N. Dong, "General Analytical Modelling for Magnet Demagnetization in Surface Mounted Permanent Magnet Machines," *IEEE Trans. Ind. Electron.*, pp. 1–1, 2018.

[7] J. Dong, J. W. Jiang, B. Howey, H. Li, B. Bilgin, A. Callegaro, and A. Emadi, "Hybrid Acoustic Noise Analysis Approach of Conventional and Mutually Coupled Switched Reluctance Motors," *IEEE Trans. Energy Convers.*, vol. PP, no. 99, pp. 1–1, 2017.

[8] J. L. Besnerais, "Fast prediction of variable-speed acoustic noise due to magnetic forces in electrical machines," in *2016 XXII International Conference on Electrical Machines (ICEM)*, Sep. 2016, pp. 2259–2265.

[9] L. Gao, H. Zheng, L. Zeng, and R. Pei, "Evaluation Method of Noise and Vibration used in Permanent Magnet Synchronous Motor in Electric Vehicle," in *2019 IEEE Transportation Electrification Conference and Expo (ITEC)*, Jun. 2019, pp. 1–4, iSSN: 2377-5483.

[10] Y. Fang and T. Zhang, "Vibroacoustic Characterization of a Permanent Magnet Synchronous Motor Powertrain for Electric Vehicles," *IEEE Trans. Energy Convers.*, vol. 33, no. 1, pp. 272–280, Mar. 2018.

[11] R. Yang, "Electrified Vehicle Traction Machine Design With Manufacturing Considerations," Ph.D. dissertation, 2017.

[12] J. Zou, H. Lan, Y. Xu, and B. Zhao, "Analysis of Global and Local Force Harmonics and Their Effects on Vibration in Permanent Magnet Synchronous Machines," *IEEE Trans. Energy Convers.*, vol. 32, no. 4, pp. 1523–1532, Dec. 2017.

[13] J. F. Gieras, *Noise of Polyphase Electric Motors*. Boca Raton, FL: CRC Press, Dec. 2005.

[14] J. Le Besnerais, "Reduction of magnetic noise in PWM-supplied induction machines - low-noise design rules and multi-objective optimisation," PhD Thesis, Lille University of Science and Technology, Lille, Nov. 2008.

[16] R. De Doncker, D. W. Pulle, and A. Veltman, *Advanced Electrical Drives*, ser. Power Systems. Dordrecht: Springer Netherlands, 2011. [Online]. Available: http://link.springer.com/10.1007/978-94-007-0181-6

Authorized licensed use limited to: TU Delft Library. Downloaded on September 06,2021 at 12:49:41 UTC from IEEE Xplore. Restrictions apply.